

# Petrography and Geochemistry of the Late Triassic Bootjack Stock (NTS 093A/12), South-Central British Columbia

Adam B. Bath<sup>1,2</sup> and James M. Logan<sup>1</sup>

**KEYWORDS:** syenite, pseudoleucite, sulphide inclusions, Mount Polley, haüyne, bornite, chalcopyrite

## INTRODUCTION

Establishing links between mineralization and causative intrusion(s) is an important and fundamental step to understanding mineralizing systems. In particular, the ability to distinguish petrological and geochemical characteristics of mineralized versus barren intrusive systems has important implications for the exploration geologist (*e.g.*, Frei, 1996).

This study investigated a Late Triassic alkalic intrusion, known as the Bootjack stock, from the south-central Canadian Cordillera. The Bootjack stock (BS) is part of the Quesnel arc complex (Fig. 1) that formed above an east-dipping subduction zone during the Late Triassic to Early Jurassic (Mortimer, 1987; Panteleyev *et al.*, 1996; Logan and Mihalynuk, 2005). Other K-rich or alkaline intrusions of similar age that occur along the Quesnel arc include the Copper Mountain intrusive rocks (Copper Mountain, Ingerbelle), White Mountain, Kruger syenite, Kamloops syenite and Iron Mask batholith (Afton, Ajax and Crescent in the south; and the Hogem batholith (Lorraine) in the north. In addition, the BS is age equivalent to syenite at Galore Creek, Copper Canyon, Zippa Mountain and Rugged Mountain, which are located within the Stikine arc terrane (Fig. 1). A number of the above intrusions are spatially and temporally coincident with Cu-Au mineralization. The BS, in particular, is spatially and temporally associated with the Cu-Au mineralizing event at Mount Polley; however, no direct links have been made between it and mineralization. The purpose of this study is to examine new major and trace element data from the BS, combined with petrographic descriptions, to determine if there are any features of the BS that could explain the alteration and mineralization events at Mount Polley. The study also compares the geochemistry of the BS with other intrusions of similar age at Mount Polley and in the Quesnel Lake area.

## REGIONAL GEOLOGY

The Bootjack stock (BS) is located in the Quesnel Lake map area (NTS 093A/12) of south-central British Colum-

bia and intrudes Triassic Nicola Group arc volcanic rocks and associated sedimentary rocks within the Quesnel Terrane (Fig. 1; Fraser, 1994; Panteleyev *et al.*, 1996; Logan and Mihalynuk, 2005). The intrusive body is closely associated, both spatially and temporally, with other alkalic intrusive phases at Mount Polley, which include diorite and plagioclase porphyry phases of the Mount Polley stock (Fraser, 1994). The BS outcrops further to the south (stratigraphically deeper) of the main mineralized centre and is separated from the Mount Polley stock and mineralization zones by a narrow belt (~2 km wide) of northwest-trending metavolcanic flows, breccia units, fine-grained bedded volcanoclastic units and a pyroxenite body, which was identified in drillcore and is located beneath Bootjack Lake (Hodgson *et al.*, 1976; Fraser, 1994). However, the northward extension of the BS is unknown, and the possibility that it intrudes rocks beneath Mount Polley cannot be ruled out.

## GEOCHRONOLOGY

### Intrusions

The relative timing of emplacement of the Bootjack and Mount Polley stocks is constrained by the presence of xenoliths. According to Fraser (1994), the BS and plagioclase porphyry include xenoliths of diorite and are therefore both younger. However, the age relationship between the BS and the plagioclase porphyry is unknown.

Estimated absolute ages suggest that the BS crystallized at  $202.7 \pm 7.1$  Ma (U-Pb date from pseudoleucite syenite; Mortensen *et al.*, 1995) or  $200.8 \pm 2.8$  Ma (U-Pb date from mafic pseudoleucite syenite; Mortensen *et al.*, 1995), and had cooled below  $300^\circ\text{C}$  by  $203.1 \pm 2.0$  Ma (Ar/Ar date from mafic pseudoleucite syenite; Bailey and Archibald, 1990), whereas the plagioclase porphyry crystallized at  $204.7 \pm 3$  Ma (U-Pb; Mortensen *et al.*, 1995). The diorite has been dated at  $201.7 \pm 0.4$  Ma (U-Pb; Mortensen *et al.*, 1995). These dates suggest that the crystallization ages of all these intrusive bodies are very similar. By combining the relative and absolute ages, it can be inferred that the BS crystallized between 202.0 and 198.0 Ma (using best U-Pb ages and errors).

### Mineralization

Brecciation and mineralization are thought to be associated with the emplacement of the alkalic intrusive bodies (Fraser, 1994); however, a definitive link between the various intrusions and mineralization has not been established. The presence of diorite clasts within the breccia (dated at  $201.6 \pm 0.5$  Ma (U-Pb zircon; Fraser, 1994) and crosscutting lamprophyre dikes that have been dated regionally at approximately 130 Ma (Mortimer *et al.*, 1990) provide

<sup>1</sup> British Columbia Ministry of Energy, Mines and Petroleum Resources, Victoria, BC

<sup>2</sup> University of Tasmania, Hobart, Tasmania, Australia.

This publication is also available, free of charge, as colour digital files in Adobe Acrobat PDF format from the BC Ministry of Energy, Mines and Petroleum Resources internet website at <http://www.em.gov.bc.ca/Mining/Geosurv/Publications/catalog/catfldwk.htm>

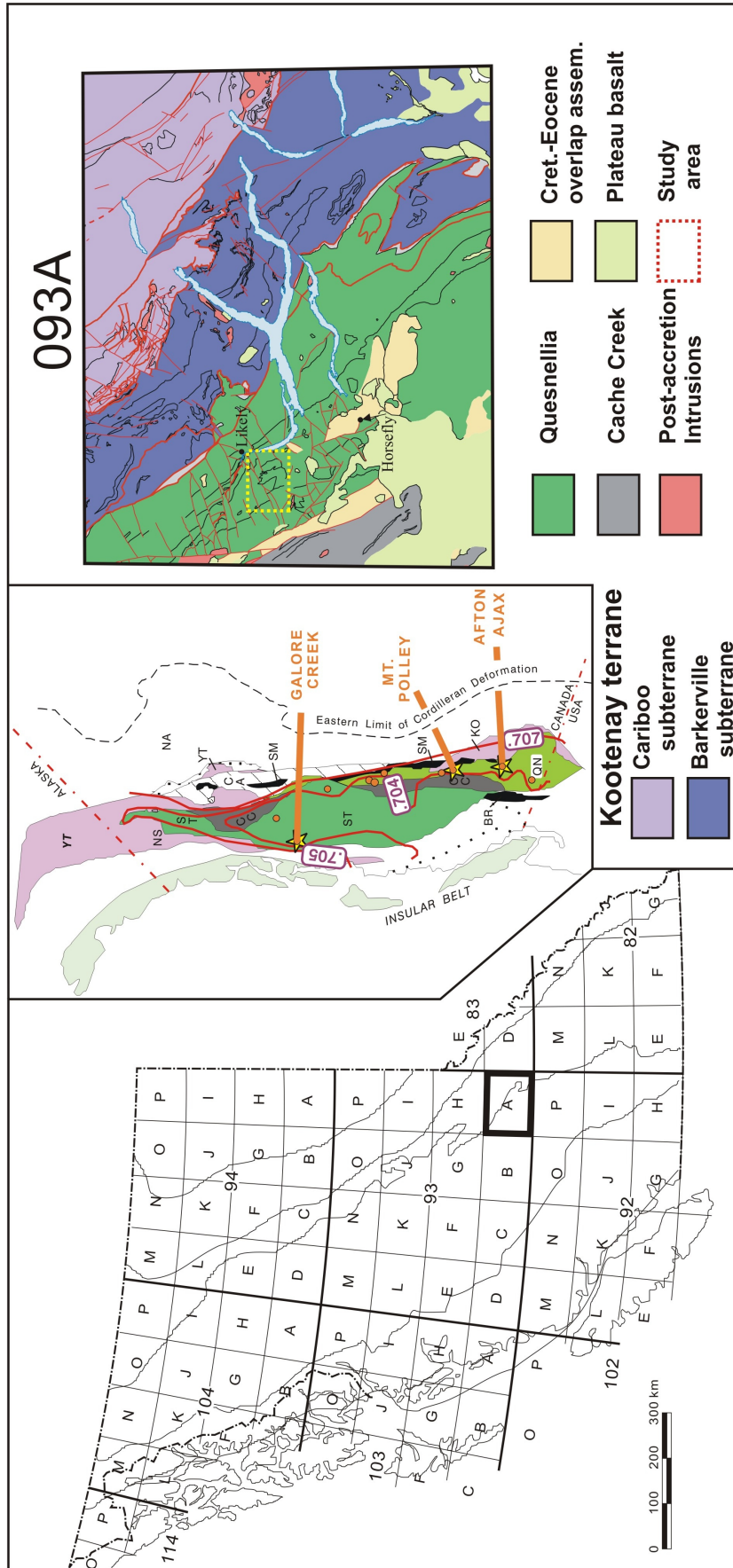


Figure 1. Location of the Mount Polley Cu-Au porphyry deposit in south-central British Columbia (NTS 0921). Inset is terrane map of the northern Cordillera (modified from Wheeler and McFeely, 1997), showing the tectonostratigraphic setting of the study area. Box on the right shows terrane relationships for NTS 093A and the project area (after Logan and Mihalynuk, 2005).

some relative age constraints. Absolute dates for mineralization have been estimated at  $184 \pm 7$  Ma for the Central zone (K-Ar biotite; Hodgson *et al.*, 1976), or more recently  $205.2 \pm 1.2$  Ma for the Northeast zone ( $Ar^{40}/Ar^{39}$  biotite; Logan and Ullrich, unpublished data, 2005) and  $220.8 \pm 1.3$  Ma for the Cariboo zone ( $Ar^{40}/Ar^{39}$  biotite; Logan and Ullrich, unpublished data, 2005).

## GEOLOGY OF THE BOOTJACK STOCK

The Bootjack stock (BS) is an elliptical, northwest-trending body that covers an area of approximately 11 km<sup>2</sup> and consists of three main rock types: 1) medium-grained sparse pseudoleucite melasyenite (MS; =15% mafic minerals); 2) orbicular pseudoleucite syenite (OPS; <15% mafic minerals); and 3) equigranular coarse to medium-grained syenite (ES; <15% mafic minerals), which contains pegmatitic zones (Fig. 2).

Medium-grained melasyenite (MS; see Fig. 2), which makes up approximately 10% of the BS, forms a rim along the margin of the stock that is estimated to be 50–300 m wide. In gradational contact with the MS and making up approximately 85% of the central region of the stock is orbicular pseudoleucite syenite. The remaining 5% of the stock consists of equigranular syenite (ES), which crops out as a thin (150 mm) dike at station ABA05 32-259 or as wider (~50 m) late intrusive phases at station ABA05 33-267, where it shows pegmatitic textures. Pegmatitic texture within the ES was also identified at other locations (*e.g.*, ABA05 41-336; Fig. 2).

Hodgson *et al.* (1976) reported igneous foliation and phenocryst distribution that impart a gross layering to the intrusion. In addition, data collected during this study suggest that isolated cumulate layering is evident at numerous outcrops (*e.g.*, ABA05 32-260 and JLO05 30-232), and trends approximately east and dips steeply to moderately to the north.

## PETROGRAPHY

Samples from the melasyenite, orbicular pseudoleucite syenite and equigranular syenite were collected, and standard thin sections, polished sections and epoxy mounts were made in order to determine mineral assemblages and identify texture, alteration assemblages and melt and fluid inclusions. Chemical tests were used to identify sodalite group minerals (sodalite, nosean and h a yne). The technique involved decomposition in nitric acid and evaporation. The precipitation of bladed colourless gypsum crystals confirmed the presence of h a yne in the samples (Deer *et al.*, 1992). To the best of the authors' knowledge, no other isotropic phase that is commonly found in nepheline syenite shows this behaviour.

Alteration is weak to moderate and assemblages are common throughout the Bootjack stock (one exception is JLO04 17-45, which is altered to sericite and cancrinite). Weakly altered samples show replacement of nepheline and h a yne with cancrinite, and of orthoclase with sericite. Mafic minerals (augite and hornblende) show reaction rims in which biotite and chlorite are common replacement phases. Some augite phases show amphibole replacement, which is evident from the relict euhedral augite crystal form with 60° and 120° cleavage angles. Minor calcite alter-

ation, identified in two samples from the OPS, accounts for <2% of the rock.

### Melasyenite

The melasyenite (MS) is light grey to dark green-grey, holocrystalline and contains crystals that are 0.5–3 mm in size. Pseudoleucite texture (pseudomorph after leucite, comprising a mixture of nepheline and orthoclase) is present in most samples, is 5–15 mm in size and light grey, and makes up 5–15% of the rock (Fig. 3C). The matrix is melanocratic, accounts for 85–95% of the rock and ranges from light grey to dark green-grey. At certain locations (*e.g.*, ABA05 34-274-4), the combined effect of a dominantly dark grey matrix and light grey orbicular pseudoleucite gives the MS a porphyritic texture. At other localities, the MS is finer grained and shows some cumulate layering (*e.g.*, JLO05 30-232).

In thin section, fresh samples consist of orthoclase (30–50%; Carlsbad twinning), nepheline (0–45%), h a yne (0–5%), biotite (0–5%) and augite (15–25%). Orthoclase, nepheline, h a yne and biotite are anhedral to subhedral and 0.5–3 mm in size, and have irregular to sharp grain boundaries, whereas augite is subhedral to euhedral and has sharp boundaries. Accessory phases include apatite, titanite and traces of fluorite; all ranging from <0.1 to 0.5 mm in size. Apatite commonly occurs as crystal inclusions within pyroxene. Opaque minerals include subhedral to anhedral magnetite, minor pyrite and tiny (<5 µm) bornite and chalcopyrite inclusions in h a yne. H a yne occurs in the matrix as subhedral crystals in approximately 50% of the MS samples.

### Orbicular Pseudoleucite Syenite

The orbicular pseudoleucite syenite (OPS) is a holocrystalline porphyritic rock consisting of pseudoleucite trapezohedrals that are 10–50 mm in diameter (Fig. 3A, B). The matrix constitutes 50–95% of the rock. It has a granitic texture and contains leucocratic phases, as well as subordinate mafic and opaque phases that are 0.5–3 mm in size. Four of the five samples are strongly dominated by pseudoleucite, which makes up 80–95% of the rock. One sample (ABA05 33-266) is more of a hybrid between OPS and ES, and contains only 50% pseudoleucite. Samples ABA05 33-266 and MMI04 18-1 differ from other samples in that their matrix includes a significant modal abundance of fresh interstitial h a yne (10–15%), which includes small (<5 µm) sulphide inclusions of bornite and chalcopyrite (Fig. 4A–D). H a yne is present but less common in other samples. It occurs both in the matrix and as a constituent of the pseudoleucite region of the rock, but is mostly devoid of inclusions and is commonly weakly altered to cancrinite.

In thin section, fresh rocks include orthoclase (50–70%; Carlsbad twinning), nepheline (15–25%), biotite (0–1%), augite (4–8%), h a yne (2–15%), hornblende (trace–10%), plagioclase (0–1%), apatite (trace–1%), magnetite (2–3%) and pyrite (trace). All phases are anhedral to subhedral in crystal form and have irregular but sharp grain boundaries. An exception to this is apatite, which is euhedral to subhedral with sharp grain boundaries and commonly occurs as crystal inclusions within clinopyroxene.

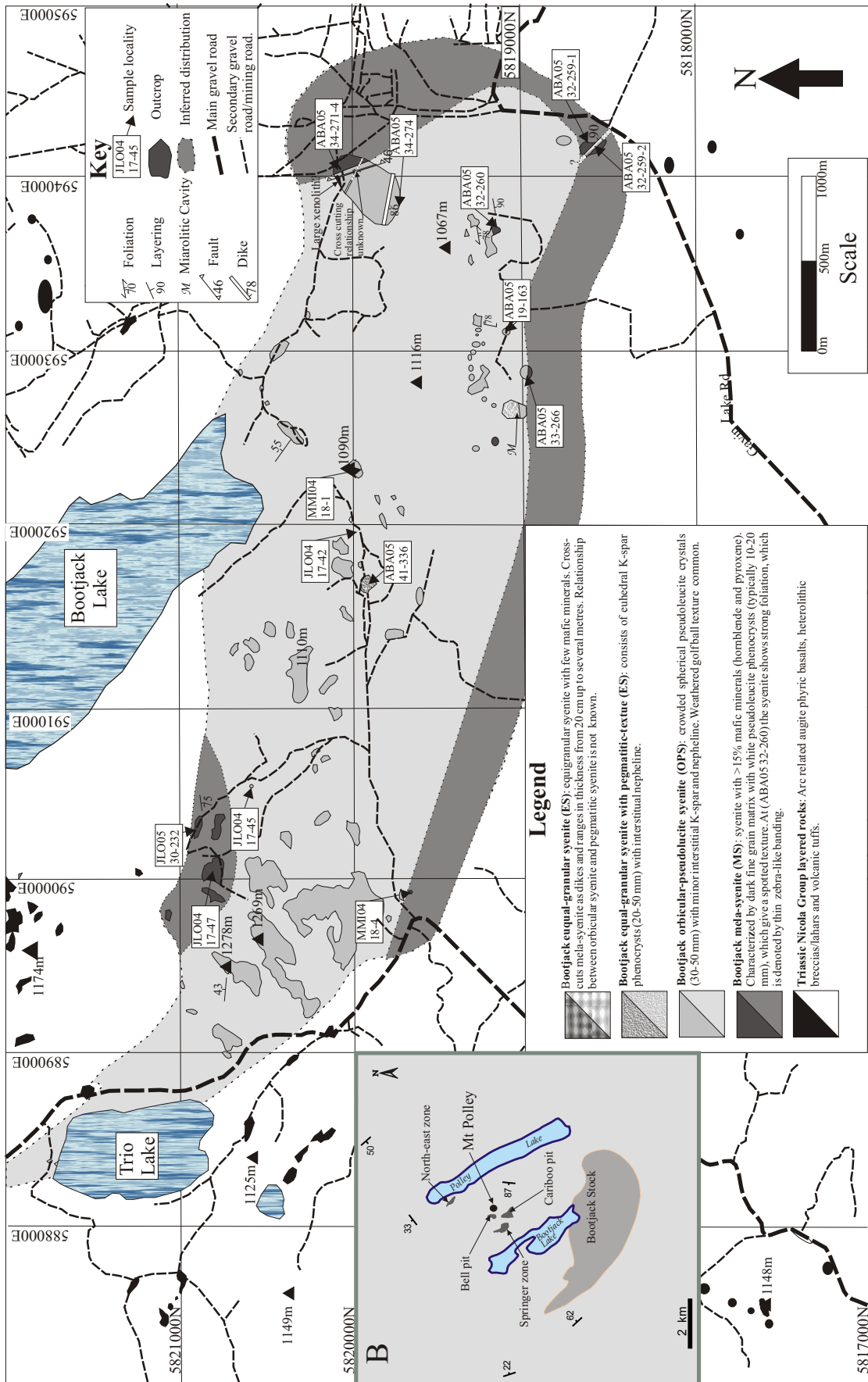


Figure 2. Geology of the Bootjack stock (NTS 093A/12), south-central British Columbia. Note that inset B shows the location of the Bootjack stock relative to Mount Polley.

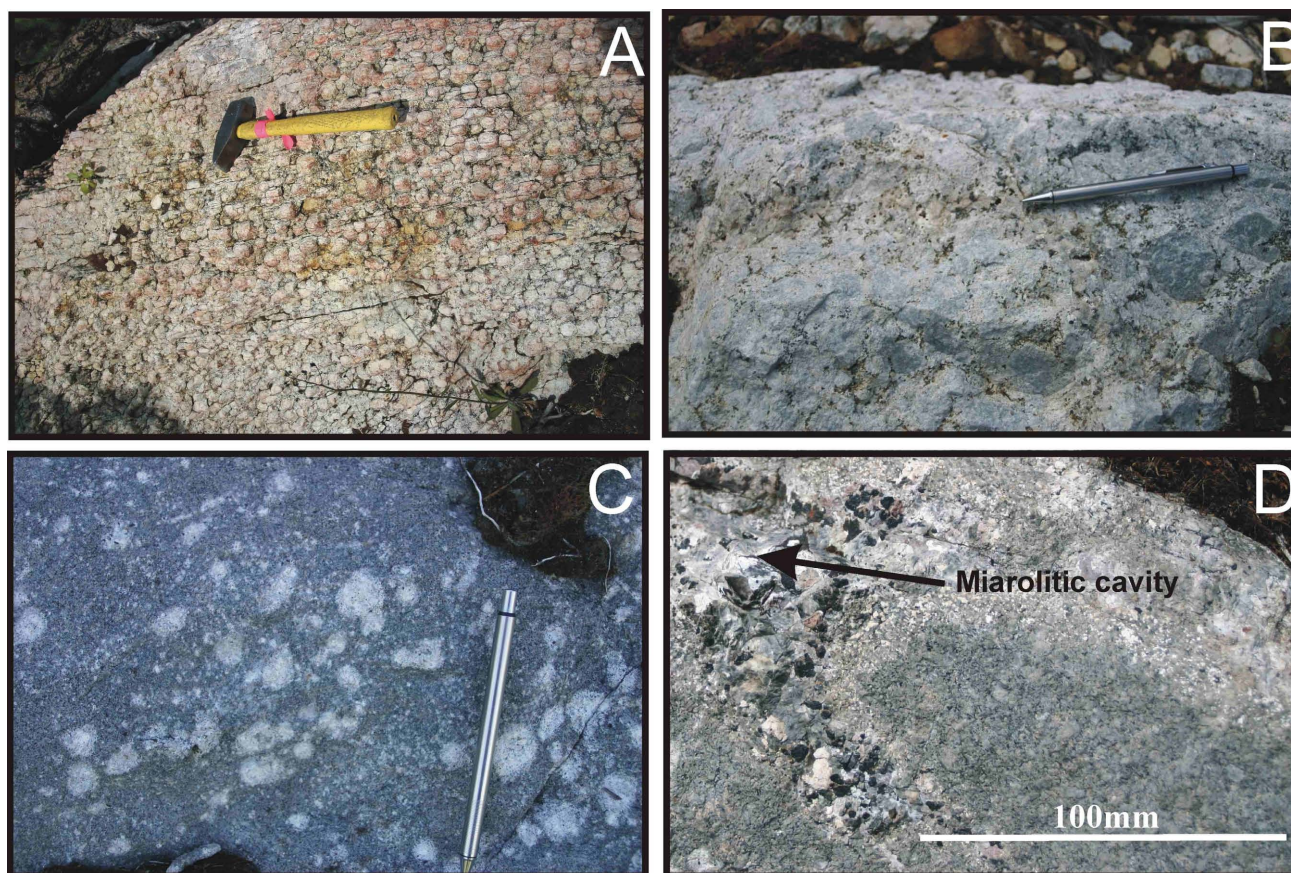


Figure 3. A) Outcrop of orbicular pseudoleucite syenite (OPS), which shows golf ball weathering. B) Fresh orbicular pseudoleucite syenite (OPS) from station ABA05 19-163. C) Melasyenite (MS) with pseudoleucite from station ABA05 32-259-1. D) Equigranular syenite (ES) with a miarolitic cavity from station ABA05 33-267. Miarolitic cavity consists of orthoclase, nepheline, magnetite, cancrinite, natrolite, sphene and fluorite.

### Equigranular Syenite

The equigranular syenite (ES) is highly variable. It ranges from light to medium grey to pink, is holocrystalline and contains crystals that are 0.5–6 mm in size (Fig. 3D). Pegmatitic texture is common (*e.g.*, ABA05 41-336).

In thin section, fresh rocks contain orthoclase (40–60%; Carlsbad twinning), nepheline (25–35%), hornblende (1–3%), augite (1–4%), h a y ne (2–7%), accessory apatite (trace) and magnetite (1%). Orthoclase, cancrinite and h a y ne are anhedral to subhedral, whereas all other phases are subhedral to euhedral. In pegmatitic ES, h a y ne is a common phases and includes sulphide inclusions of bornite and chalcopyrite.

### MELT INCLUSIONS

Numerous types of melt and fluid inclusions were identified in apatite, sphene, pyroxene, hornblende and h a y ne (usually less than 20  $\mu\text{m}$  in size). Inclusions hosted in apatite, sphene, hornblende and pyroxene are dominated by silicate glass with small shrinkage bubble(s) and aqueous fluid inclusions, whereas inclusions in h a y ne consist of sulphide minerals and unknown light green transparent material. This study will focus only on inclusions hosted in interstitial h a y ne.

Three types of coexisting primary melt inclusions were identified in h a y ne (types 1–3). Type 1 consists entirely of intergrown bornite and chalcopyrite (Fig. 4D). The bornite/chalcopyrite ratio is highly variable and, in many samples, inclusions exist entirely of bornite or chalcopyrite. Inclusions are mostly <5  $\mu\text{m}$  in diameter and are irregular to globular.

Type 2 inclusions consist entirely of birefringent material (silicate, sulphate and carbonate?) and rarely contain a small shrinkage bubble (Fig. 4C). Type 2 inclusions range in shape from irregular to cubic to tabular and are mostly <5  $\mu\text{m}$  in diameter.

Type 3 inclusions are composite inclusions comprising sulphide minerals (chalcopyrite and bornite), birefringent material (type 2 composition) and rarely a small shrinkage bubble (Fig. 4C). The ratio of sulphide minerals to birefringent material is highly variable. Type 3 inclusions are mostly <10  $\mu\text{m}$  in diameter and range from irregular to globular in shape.

### GEOCHEMISTRY

#### Analytical Methods

Fourteen samples from the Bootjack syenite were analyzed for major, minor and trace elements. Six samples

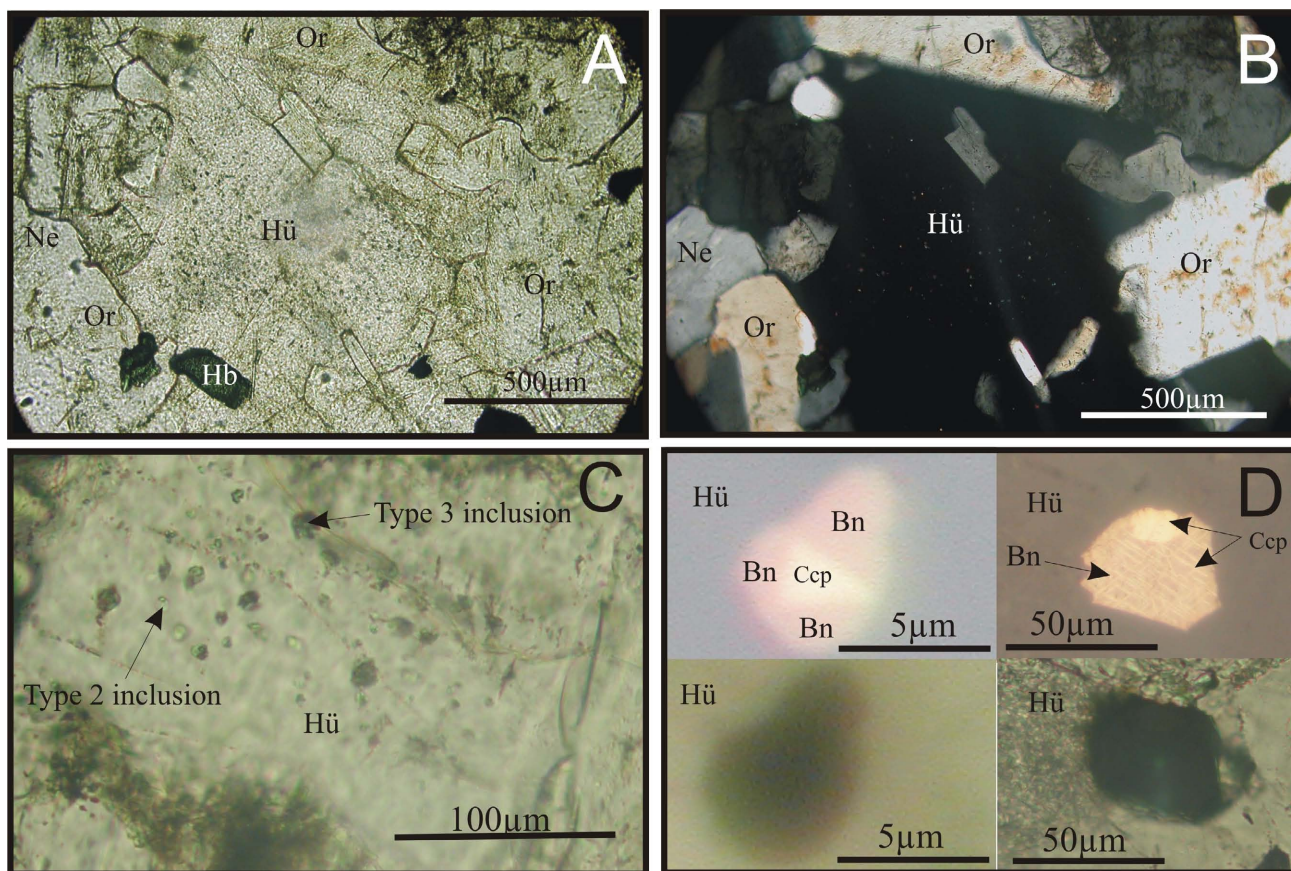


Figure 4. A) Photomicrograph of sample ABA05 33-266 (OPS) under plane-polarized light. Note the presence of orthoclase (Or), nepheline (Ne), haüyne (Hü) and hornblende (Hb). B) Photomicrograph of sample ABA05 33-266 (OPS) under cross-polarized light. Note the interstitial haüyne and the small birefringent inclusions (type 2 and 3) within haüyne (silicate, sulphate or carbonate material?). C) Type 2 and 3 inclusions in haüyne. D) Type 1 inclusions under plane-polarized light (bottom) and reflected light (top). The latter shows bornite (Bn) intergrown with chalcopyrite (Ccp), which is a common feature of type 1 inclusions.

were collected from the MS, six from the OPS and two from the ES. All samples were crushed and milled at the BC Geological Survey using a Cr-Fe plated jaw crusher, a tungsten carbide mill for major oxides (plus select trace elements) and a Cr-Fe mill for trace elements. In all cases, samples were free of xenoliths and weathered surfaces. For quality control, several hidden duplicates were included in the batch of samples to enable estimation of analytical precision, and several standard rock powders were included to allow estimation of analytical accuracy (Tables 1, 2).

Major oxides and Ba were determined by analyzing a fusion disc with a Siemens SRS-200 sequential X-ray fluorescence spectrometer (XRF) at Cominco Research Labs, Vancouver. Select trace elements (Rb, Sr, Y, Zr, Nb) were also analyzed by XRF using a pressed powdered pellet, and FeO was analyzed by titration at Cominco Research Labs. Analysis of rare earth elements (REE), Y, Th, Zr, Nb, Ba, Hf and Ta was carried out using the sodium peroxide sinter digestion technique and analyzed with a Hewlett Packard 4500plus ICP-MS at Memorial University, Newfoundland (MUN). The elements Mo, Cu, Pb, Zn, Ag, Ni, Co, As, U, Bi and W were all analyzed with a Perkin Elmer Elan 9000 ICP-MS at ACME Analytical Laboratories Ltd., Vancouver (four-acid [HClO<sub>4</sub>, HNO<sub>3</sub>, HCl and HF] digest ultra-trace method). Gold was determined by fire assay and ICP-ES (SpectroCircus Vision) at ACME.

It is important to note that trace elements Ba, Nb, Y and Zr were analyzed using both XRF and ICP-MS. However, according to P. King of MUN (pers. comm., 2005) the use of Ba, Nb, Ta, Hf and Zr data from the ICP-MS method should be treated only semiquantitatively (particularly Ba, Hf and Zr), as development work is still in progress to improve the reliability of these particular elements at MUN. Therefore, only XRF data for Zr and Nb will be used in this manuscript for interpretation purposes. Cominco Research Labs indicated that Ba values detected using XRF should also be treated with caution, so Ba has not been used in this manuscript for interpretation purposes. However, it is interesting to note that the comparison between the XRF and ICP-MS methods showed no correlation for Ba (*i.e.*,  $R^2 = <0.1$ ), a very weak correlation for Nb ( $R^2 = 0.28$ , slope = 0.89), moderate correlation for Y ( $R^2 = 0.51$ , slope = 0.84) and a moderate to strong correlation for Zr ( $R^2 = 0.72$ , slope = 1.15). In the case of Zr, Nb and Y, some of the error can be attributed to the difference in detection limit between the two methods (see Tables 1, 2). This is particularly important for Y and Nb, where the measured values are not significantly greater than the detection limit for the XRF method (3 ppm).

**TABLE 1. MAJOR OXIDE AND SELECT TRACE ELEMENT GEOCHEMISTRY FROM THE BOOTJACK STOCK AND OTHER INTRUSIONS FROM THE QUESNEL LAKE MAP AREA. ALL ELEMENTS WERE ANALYZED AT COMINCO RESEARCH LABS, VANCOUVER. ABBREVIATIONS FOR ANALYTICAL METHODS: XRF1, FUSED-DISC X-RAY FLUORESCENCE; TIT, HF DIGESTION - TITRATION; XRF2, PRESSED-PELLET X-RAY FLUORESCENCE. ROCK TYPE AND MINERAL ABBREVIATIONS: OPS, ORBICULAR PSEUDOLEUCITE SYENITE; MS, MELASYTE; ES, EQUIGRANULAR SYENITE; MONZ, MONZONITE; SYN, SYENITE; DIO, DIORITE; HBL, HORNBLLENDE; PX, PYROXENE; K-SPAR, K-FELDSPAR; MEG, MEGACRYSTIC. NOTE THAT SAMPLES ARE FROM UTM ZONE 10**

Field Number	Bootjack Stock	LAT	LONG	Element Units Method	Deletion Limit	SiO2 %	TiO2 %	Al2O3 %	Fe2O3 %	FeO %	MnO %	MgO %	CaO %	Na2O %	K2O %	P2O5 %	Ba* %	LOI %	Total %	Nb ppm	Rb ppm	Sr ppm	Y ppm	Zr ppm	XRF1		XRF2	
																									XRF1	XRF2	XRF1	XRF2
591968	5819970 OPS					53.72	0.14	22.94	0.91	0.61	0.05	0.43	1.4	5.26	11.8	0.07	0.18	2.11	99.69	bd	280	1487	bd	16				
JLO04-17-42						57.22	0.1	23.68	0.64	0.34	0.02	0.17	0.64	0.77	13.77	0.01	0.08	2.32	99.8	5	248	112	7	48				
590530	5820600 OPS					50.24	0.43	20.73	3.86	1.85	0.2	2.22	4.05	2.75	7.38	0.23	0.41	3.96	98.52	3	119	7504	bd	113				
JLO04-17-47						51.79	0.38	20.63	3.44	1.41	0.18	1.69	4.98	3.67	7.23	0.25	0.18	3.42	99.25	6	111	2592	10	21				
JLO05 30-232						54.08	0.12	22.31	1.1	0.45	0.07	0.23	0.89	6.65	10.39	0.01	0.04	2.81	99.21	10	315	626	7	48				
MM104-18-1						52.04	0.36	21.37	2.89	1.51	0.15	1.32	4.13	6.34	7.3	0.25	0.2	1.07	99.1	4	97	2474	12	53				
MM104-18-4						53.2	0.18	22.61	1.55	0.73	0.05	0.69	2.02	4.55	12.39	0.14	0.16	1.45	99.74	4	283	1553	bd	9				
ABA05 19-163						53.29	0.31	21.79	2.12	1.3	0.12	0.93	3.02	5.53	8.93	0.18	0.25	1.77	99.54	5	144	2621	3	bd				
ABA05 32-259-1						52.52	0.3	21.62	2.45	1.23	0.15	1.07	3.09	5.15	8.36	0.18	0.18	3.16	99.46	4	82	2663	6	23				
ABA05 32-259-2						52.06	0.41	21.21	3.29	2.02	0.18	1.64	5.44	6.9	5.01	0.31	0.23	1.05	99.75	3	57	3665	5	57				
ABA05 32-260						54.65	0.17	22.56	1.36	0.69	0.09	0.38	1.47	7.03	9.44	0.05	0.12	1.7	99.71	5	167	1582	bd	17				
ABA05 33-266						50.95	0.33	21.73	2.76	1.34	0.14	1.32	3.9	5.01	8.78	0.28	0.26	2.62	99.42	bd	105	3733	bd	14				
ABA05 34-271-4						53.24	0.2	22.27	1.62	0.72	0.07	0.79	1.97	4.82	11.22	0.15	0.18	2.47	99.72	3	254	1651	bd	bd				
ABA05 34-274						54.27	0.15	23.02	1.32	0.61	0.1	0.31	1.33	7.42	8.68	0.05	0.13	2.48	99.87	3	121	1408	44	39				
ABA05 41-336						60	0.41	18.37	2	0.96	0.01	0.72	2.48	6.03	6.07	0.07	0.17	2.18	99.58	7	72	246	25	130				
Bullion pit						46.65	1.2	16.54	6.36	4.94	0.17	5.07	10.46	3.01	2	0.36	0.1	2.24	99.65	3	31	602	23	43				
JLO04-11-4a						58.04	0.77	18.7	3.08	1.15	0.01	1.05	3.11	6.69	4.25	0.11	0.14	2.83	99.63	6	96	419	21	123				
JLO04-11-4b																												
ABA05 22-180																												
MIT-Poley mine																												
JLO04-20-70b						49.47	0.77	18.51	5.3	2.49	0.18	2.81	8.27	4.09	3.9	0.43	0.15	2.59	99.24	4	51	1277	24	64				
JLO04-20-73						50.25	0.81	17.34	5.58	3.5	0.18	3.64	8.42	3.51	3.57	0.38	0.24	1.73	99.54	bd	57	959	24	62				
JLO04-23-100						56.2	0.43	18.93	3.7	1.17	0.23	1.41	4.36	4.03	6.63	0.18	0.15	1.6	99.16	6	124	1175	17	92				
JLO04-24-111						53.66	0.68	18.04	3.17	3.41	0.18	2.88	5.46	4.86	3.44	0.27	0.19	2.69	99.31	bd	52	1049	24	85				
MM104-13-6						48.33	0.75	18.3	6.14	3.25	0.2	4.01	10.19	3.17	2.5	0.34	0.18	1.76	99.49	bd	28	852	19	47				
MM104-23-5						51.74	0.69	18.01	6.35	1.11	0.18	2.97	7.92	4.98	1.32	0.23	0.02	4.01	99.66	bd	17	302	25	58				
ABA05 28-226						54.93	0.5	18.4	3.39	1.55	0.15	1.42	6.21	5.13	4.75	0.23	0.13	2.56	99.35	4	94	1054	18	84				
ABA05 28-227						55	0.5	18.53	3.31	1.66	0.11	1.45	5.8	5.34	4.38	0.2	0.13	3.04	99.45	4	92	1178	21	85				
ABA05 28-229						49.45	0.77	18.29	5.74	2.02	0.2	2.96	8.01	4.3	4	0.44	0.14	3.21	99.53	5	70	1159	23	56				
ABA05 41-335						50.93	0.81	17.95	6.05	1.88	0.2	2.92	7.23	4.21	3.69	0.4	0.18	2.87	99.32	bd	63	1582	18	40				
ABA05 16-130						51.72	0.69	17.63	5.03	2.53	0.18	3.09	7.69	4.19	3.3	0.37	0.09	2.83	99.34	4	59	893	23	63				
JLO05 14-113						52.7	0.62	18.55	5.12	2.45	0.18	2.85	6.51	3.7	4.55	0.31	0.19	1.93	99.66	bd	91	1234	21	62				
Shiko Lake																												
JLO04-21-83a						53.11	0.54	18.05	3.2	2.27	0.09	2.96	6.48	6.38	1.32	0.4	0.05	4.11	99.22	bd	16	1283	15	52				
JLO04-21-83b						59.04	0.36	17.95	2.67	1.2	0.05	1.3	3.48	4.94	6.34	0.18	0.16	1.41	99.22	6	70	665	21	85				
JLO04-21-85a						51.5	0.91	17.5	4.54	3.65	0.15	4.15	7.25	3.99	3.32	0.49	0.1	1.6	99.56	4	52	1000	18	46				
JLO04-21-85b						61.34	0.3	15.69	3.77	1.91	0.05	1.39	2.16	3.51	7.63	0.14	0.13	1.04	99.28	5	103	428	15	82				
ABA05 12-95						49.58	0.82	16.75	6.43	3.18	0.14	4.84	8.27	3.48	3.23	0.52	0.12	2.1	99.46	3	65	940	12	20				
ABA05 21-172						50.93	0.77	16.7	5.16	4.4	0.18	4.3	8.73	3.28	3.5	0.43	0.11	1.21	99.7	bd	64	932	16	44				
ABA05 25-202						51.43	0.64	16.46	4.04	2.89	0.14	3.89	8.47	3.73	3.39	0.37	0.16	3.42	99.03	3	51	756	18	46				
Misc																												
JLO05 6-30						48.99	0.56	12.64	4.99	5.63	0.18	7.76	9.96	2.1	3.97	0.46	0.09	2.02	99.35	bd	103	951	9	26				
JLO05 15-117						51.65	0.64	18.3	6.06	1.15	0.18	2.48	6.73	5.71	2.65	0.38	0.12	3.43	99.48	bd	36	1719	20	54				
JLO05 34-260						55.88	0.46	18.12	3.86	2.16	0.12	2.91	4.4	6.01	3.25	0.28	0.1	1.98	99.53	bd	52	827	19	48				
ABA05 35-280						49.38	0.85	17.2	2.16	7.07	0.15	4.42	8.35	2.86	3.61	0.37	0.14	3.29	99.85	bd	106	802	19	37				
GC																												
CANMET SY4						49.69	0.28	20.59	3.11	2.69	0.10	0.51	7.98	7.03	1.60	0.11	0.03	5.41	99.10	10	54	1212	114	508				
CANMET SY4						49.9	0.287	20.69	3.35	2.86	0.108	0.54	8.05	7.1	1.66	0.131	0.034	4.56	99.10	13	55	1191	119	517				
JLO 5-20						48.93	0.51	16.43	6.43	1.88	0.17	5.55	7.42	6.32	0.92	0.62	0.12	4.42	99.72	bd	17	1040	16	38				

**TABLE 2. TRACE ELEMENT DATA FOR THE BOOTJACK STOCK AND OTHER ALKALIC INTRUSIONS IN THE QUESNEL LAKE MAP AREA. NOTE THAT ELEMENTS AU TO W (LEFT SIDE OF TABLE) WERE ANALYZED AT ACME ANALYTICAL LABORATORIES LTD., VANCOUVER (ACME), WHEREAS ELEMENTS Y TO TH (RIGHT SIDE OF TABLE) WERE ANALYZED AT MEMORIAL UNIVERSITY, NEWFOUNDLAND (MUN). ABBREVIATIONS FOR ANALYTICAL METHODS: FAI, LEAD COLLECTION FIRE ASSAY – ICPEs FINISH; TICP, FOUR-ACID DIGESTION – INDUCTIVELY COUPLED PLASMA – EMISSION/MASS SPECTROMETRY; PIMS, PEROXIDE FUSION – ICP-MS. ALSO NOTE THAT THE HIDDEN STANDARD FOR ACME WAS GSB TILL 99/GRX1, WHEREAS THE HIDDEN STANDARD FOR MUN WAS CANIMET SY4 (GREY BACKGROUND). MMI04 21-1 WAS USED AS A HIDDEN REPEAT FOR ACME, WHEREAS SAMPLE ABA05 32-259-1 WAS USED FOR MUN (GREY BACKGROUND)**

Element	Au	Mo	Cu	Pb	Zn	Ag	Ni	Co	As	U	Bi	W	Y	Zr	Nb	Ba	La	Ce	Pr	Nd	Sm	Eu	Gd	Tb	Dy	Ho	Er	Tm	Yb	Lu	Hf	Ta	Th				
Method	ppb	ppm	TICP	TICP	ppm	ppb	TICP	TICP	ppm	ppm	TICP	TICP	ppm	ppm	ppm	ppm	ppm	ppm	ppm	ppm	ppm	ppm	ppm	ppm	ppm	ppm	ppm	ppm	ppm	ppm	ppm	ppm	ppm				
Detection Limit	1	0.05	0.02	0.02	0.1	20	0.1	0.2	0.2	0.1	0.04	0.1	0.004	0.04	0.03	0.08	0.01	0.01	0.01	0.00	0.03	0.01	0.01	0.02	0.00	0.03	0.00	0.01	0.00	0.01	0.00	0.02	0.04	0.01			
<b>Bootjack Stock</b>																																					
JLO04-17-42	4	0.22	54.36	6.04	29.6	32	0.9	3.7	28.0	0.4	bd	0.4	2.757	12.20	1.22	1939.29	3.90	6.29	0.76	2.98	0.57	0.22	0.55	0.08	0.50	0.10	0.30	0.04	0.32	0.05	0.28	0.05	0.51				
JLO04-17-45	11	0.18	51.50	7.07	64.6	44	0.5	1.4	11.8	0.7	bd	0.7	4.940	34.14	3.82	843.72	6.03	9.17	1.04	3.66	0.66	0.20	0.66	0.11	0.70	0.17	0.58	0.10	0.70	0.10	0.67	0.20	2.88				
JLO04-17-47	5	1.05	29.05	11.88	94.2	23	3.8	16.9	11.6	0.6	bd	1.5	9.943	34.81	2.82	8821.45	10.42	18.21	2.29	9.50	1.93	0.50	1.93	0.29	1.83	0.38	1.14	0.17	1.20	0.17	0.93	0.12	1.02				
JLO05 30-232	5	0.88	14.39	11.88	88.1	bd	1.4	13.4	9.1	1.5	bd	0.6	11.673	60.62	5.00	2291.65	13.12	23.04	2.87	11.86	2.41	0.76	2.36	0.35	2.16	0.44	1.34	0.20	1.40	0.21	1.50	0.23	2.53				
MMI04-18-1	6	0.87	43.54	13.62	53.3	47	0.7	2.3	9.9	1.4	bd	0.3	3.532	38.15	7.37	489.19	5.35	8.69	0.98	3.52	0.63	0.19	0.59	0.09	0.59	0.13	0.41	0.07	0.52	0.07	0.74	0.32	2.28				
ABA05 19-163	bd	0.26	78.60	6.97	38.3	57	1.5	6.7	48.2	0.4	bd	0.3	3.464	14.23	1.02	1902.49	4.82	8.09	0.98	3.98	0.78	0.32	0.73	0.10	0.61	0.13	0.38	0.06	0.34	0.06	0.31	0.04	0.44				
ABA05 32-259-1	bd	1.79	50.78	9.23	68.9	bd	1.2	8.4	1.1	0.1	bd	0.7	7.815	23.86	1.31	3338.77	9.25	15.85	1.97	8.11	1.68	0.64	1.60	0.24	1.47	0.30	0.87	0.13	0.83	0.13	0.68	0.06	0.45				
ABA05 32-259-2	3	0.89	28.47	14.08	85.6	22	0.8	9.4	4.4	1.5	bd	0.3	9.546	57.26	4.49	2998.02	11.12	18.88	2.27	8.96	1.80	0.65	1.73	0.27	1.72	0.36	1.10	0.17	1.19	0.18	1.33	0.20	1.64				
ABA05 32-260	bd	1.97	108.67	13.93	104.7	70	1.4	16.0	2.8	0.6	bd	0.9	12.563	52.04	4.68	3054.12	15.86	27.37	3.35	13.73	2.70	0.93	2.60	0.38	2.36	0.48	1.40	0.21	1.40	0.21	1.34	0.19	1.24				
ABA05 32-266	8	1.61	47.32	17.03	55.4	43	0.7	3.5	11.4	1.3	bd	0.5	6.702	69.01	3.86	1483.77	8.77	13.97	1.49	5.13	0.98	0.38	0.95	0.16	1.07	0.23	0.81	0.13	0.94	0.14	1.29	0.16	3.71				
ABA05 34-271-4	2	2.15	185.71	12.22	81.1	265	1.4	11.1	1.9	0.7	bd	0.5	8.496	38.47	3.47	4935.31	13.09	21.82	2.55	10.18	1.93	0.69	1.84	0.25	1.56	0.32	0.94	0.14	0.97	0.14	0.89	0.16	2.18				
ABA05 34-274	3	0.17	66.19	5.50	29.5	35	0.7	5.1	3.8	0.2	bd	0.1	4.116	13.28	0.83	2089.36	6.14	10.59	1.27	5.18	0.99	0.33	0.92	0.13	0.78	0.15	0.45	0.07	0.45	0.07	0.35	0.04	0.38				
ABA05 41-336	5	0.90	49.85	18.52	61.2	42	0.3	3.0	8.7	2.4	bd	0.3	5.469	74.19	4.34	1532.70	8.64	12.78	1.36	4.72	0.86	0.33	0.78	0.13	0.85	0.19	0.66	0.11	0.85	0.13	1.45	0.13	4.05				
<b>Bullion pit</b>																																					
JLO04-11-4a	17	0.59	806.22	1.96	9.5	361	1.2	5.1	10.0	1.4	bd	0.4	16.256	134.73	5.79	2209.56	13.85	27.17	3.76	13.31	2.57	0.77	2.70	0.44	2.85	0.59	1.82	0.29	2.06	0.31	2.98	0.33	4.54				
JLO04-11-4b	5	0.69	68.87	1.58	60.1	33	10.2	36.6	9.5	0.7	bd	0.3	16.664	60.59	3.21	1205.73	9.11	19.67	2.76	12.80	3.06	1.03	3.54	0.55	3.41	0.67	1.90	0.27	1.79	0.26	1.66	0.14	1.27				
<b>MT Polley mine</b>																																					
JLO04-20-70b	3	1.22	145.30	8.82	108.9	99	1.9	22.2	6.8	1.2	0.4	0.5	19.708	70.78	3.23	1712.93	10.79	20.13	2.70	12.26	2.95	0.99	3.61	0.59	3.78	0.77	2.29	0.33	2.23	0.30	1.78	0.15	1.64				
JLO04-20-73	8	0.78	185.44	4.82	89.0	48	2.9	28.4	9.1	0.6	bd	0.2	20.842	71.21	2.70	2761.67	8.97	18.54	2.63	12.28	3.07	1.00	3.85	0.63	4.06	0.82	2.37	0.34	2.28	0.32	1.96	0.12	1.20				
JLO04-21-100	5	2.34	102.26	35.97	266.4	389	2.2	12.5	12.4	1.7	0.12	1.7	15.692	91.22	6.69	1876.47	15.30	27.29	3.51	14.55	2.99	0.89	3.10	0.49	3.05	0.61	1.84	0.28	1.91	0.26	2.24	0.23	3.85				
JLO04-24-111	6	0.88	146.97	3.16	77.6	84	3.5	16.8	3.2	0.6	bd	0.4	21.852	98.37	5.57	2411.25	8.92	18.41	2.61	11.99	2.94	1.02	3.65	0.62	4.03	0.84	2.56	0.39	2.64	0.38	2.39	0.17	1.28				
MMI04-13-6	6	0.75	203.10	5.16	92.3	82	4.6	30.4	2.9	0.7	bd	0.2	16.708	51.95	4.78	2190.61	7.57	15.33	2.18	10.30	2.56	0.91	3.13	0.51	3.28	0.66	1.92	0.28	1.82	0.26	1.41	0.13	0.96				
MMI04-23-5	bd	1.28	11.01	6.20	115.0	51	0.4	15.9	5.4	0.8	bd	0.3	17.397	59.21	2.30	299.20	6.81	13.82	2.08	10.03	2.65	0.95	3.25	0.54	3.42	0.71	2.09	0.30	1.97	0.28	1.58	0.11	1.39				
ABA05 28-226	5	8.31	38.28	12.86	125.8	134	0.8	6.5	9.8	1.3	bd	2.6	18.661	96.64	4.38	1672.12	11.88	21.75	2.78	12.05	2.81	0.92	3.02	0.51	3.39	0.70	2.19	0.33	2.21	0.35	2.46	0.18	2.12				
ABA05 28-227	7	5.97	19.00	11.23	59.0	112	1.1	3.2	11.4	1.4	0.13	1.7	19.536	98.06	4.32	1779.47	13.18	24.36	3.15	13.37	3.13	1.00	3.46	0.54	3.65	0.76	2.31	0.35	2.36	0.36	2.52	0.21	2.00				
ABA05 28-229	6	0.98	131.78	7.96	109.5	80	1.8	21.9	5.0	1.0	bd	0.4	21.134	75.77	3.63	1848.25	11.95	22.47	3.05	13.68	3.43	1.18	4.00	0.64	4.13	0.87	2.53	0.36	2.39	0.35	2.05	0.16	1.75				
ABA05 41-335	bd	1.28	62.48	7.21	139.0	52	1.8	20.6	9.5	1.0	0.08	0.4	20.649	80.39	5.08	2330.76	13.05	24.56	3.00	14.61	3.56	1.15	4.02	0.63	3.97	0.83	2.39	0.35	2.30	0.35	2.20	0.17	1.84				
ABA05 16-130	bd	0.44	63.82	8.97	95.3	71	7.1	21.8	4.1	1.2	0.05	0.2	19.715	84.02	3.78	1204.13	16.52	29.61	3.80	16.16	3.59	1.18	3.89	0.60	3.78	0.78	2.30	0.34	2.29	0.34	2.10	0.17	2.32				
<b>Shilko Lake</b>																																					
JLO04-21-83a	27	0.37	256.50	4.65	36.3	96	4.1	13.7	7.0	0.9	bd	0.6	10.532	58.39	2.09	523.37	6.94	13.47	1.84	8.26	1.88	0.73	2.12	0.33	2.06	0.41	1.18	0.18	1.19	0.18	1.54	0.09	1.26				
JLO04-21-83b	140	0.42	137.68	4.17	25.8	130	1.8	5.8	2.2	2.5	bd	0.2	11.933	103.51	6.67	1879.33	10.05	19.35	2.40	9.64	1.97	0.61	2.06	0.33	2.16	0.45	1.37	0.22	1.57	0.23	2.29	0.24	3.36				
JLO04-21-85a	33	0.57	219.09	5.83	57.8	108																															

## Major Oxides and Normative Mineralogy

Major oxides data can be found in Table 1. These data are presented in order to 1) classify rocks from the BS using the IUGS system (Streckeisen, 1976); 2) determine if fractionation trends exist between the various rock types; and 3) compare the BS with other regional alkalic intrusions from the Quesnel Lake area (*i.e.*, Mount Polley stock, Bullion Pit, Gavin Lake, Shiko Lake, QR mine and Bootjack Lake pyroxenite), which are either assumed or known to be similar in age to the BS (Table 1; Fig. 5).

For classification purposes, CIPW normative calculations were used to plot each sample on a Streckeisen diagram (Fig. 6). Plots show that the BS is nepheline normative and ranges from Foid syenite to Foid monzonite. Exceptions to this are the finer grained MS and more altered OPS sample (JLO04 17-42) from the northeastern margin of the intrusion, which have normative compositions resembling Foid-bearing alkali-feldspar syenite to Foid-bearing syenite (Fig. 6; Streckeisen, 1976). Other discrimination plots used include the Ne-Q-Ka (nepheline-quartz-kalsilite) diagram (Fig. 7), which demonstrates that BS rocks plot in the leucite field (Rollinson, 1993), and the total alkali versus SiO<sub>2</sub> (TAS) plot, which demonstrates that the BS ranges from basic to intermediate (between 45 and 67 wt% SiO<sub>2</sub>) and plots in the alkaline field (Wilson, 1989; Fig. 5J).

To test if fractionation trends exist between the various phases of the BS, MgO was selected as a common abscissa on a series of bivariate diagrams (Fig. 5A–I). The variation diagrams show that rocks of the BS are depleted in MgO (0.17–2.22 wt%) compared to other regional intrusions. The ES and the OPS have lower MgO values (0.17–1.07 wt% and 0.23–0.79 wt%, respectively) and the MS has higher MgO values (0.93–2.22 wt%), which directly reflects the mafic component of the rock (*i.e.*, rocks with greater than ~1 wt% MgO tend to have =15% mafic minerals). For plots of TiO<sub>2</sub>, FeO<sub>T</sub>, CaO and P<sub>2</sub>O<sub>5</sub> versus MgO (Fig. 5), strong positive linear trends exist, which is consistent with the crystallization (subtraction) of pyroxene (Mg, Ca and Fe), Fe and Ti-oxides, amphibole (Ca), minor plagioclase (Ca) and apatite (Ca and P) during fractionation. In contrast, Al<sub>2</sub>O<sub>3</sub>, SiO<sub>2</sub> and total alkali show strong negative linear correlations with MgO (Fig. 5), whereas K<sub>2</sub>O shows a weak negative correlation with SiO<sub>2</sub> and Na<sub>2</sub>O shows no correlation. Overall, OPS rocks are the most fractionated and MS are the least fractionated.

Bivariate diagrams employing MgO are also used here to compare the BS with other alkalic intrusive phases from the Quesnel Lake area. The bivariate diagrams demonstrate that a single moderate to strong correlation exists for MgO versus TiO<sub>2</sub>, FeO<sub>T</sub>, CaO and P<sub>2</sub>O<sub>5</sub> for all intrusive rocks, with the BS at the most evolved end of the spectrum and the pyroxenite at the least evolved end. In the case of Al<sub>2</sub>O<sub>3</sub>, SiO<sub>2</sub> and K<sub>2</sub>O, there is a single trend for the regional intrusive rocks that differs from the BS. Alumina and K<sub>2</sub>O are both significantly more enriched for the BS when compared to regional intrusions with equivalent MgO, whereas the BS is depleted in SiO<sub>2</sub> compared to regional intrusions with equivalent MgO. It is important to note that, although the regional intrusions are more enriched in SiO<sub>2</sub> compared with the BS, they are almost always silica undersaturated and tend to plot within the Foid-bearing syenite or monzonite field on the Streckeisen diagram (Fig. 6). One other significant difference between the BS and regional in-

trusions is that BS rocks plot in the leucite field on the Ne-Q-Ka diagram, whereas all regional intrusions plot in the feldspar field (Fig. 7).

## Trace and Rare Earth Elements

Trace element data for the BS and regional intrusions can be found in Table 2. The data and various graphs are presented in order to 1) determine if fractionation trends exist for trace elements versus MgO; 2) compare primordial mantle – normalized data from the BS with other regional intrusions on a spider diagram; and 3) determine if any correlations exist between Cu, Au, Ag and other metals of commercial value.

Rocks from the BS show a positive correlation for MgO versus REE ( $R^2 = 0.53–0.75$ ), Y ( $R^2 = 0.67$ ), Ni ( $R^2 = 0.60$ ), Zn ( $R^2 = 0.54$ ), W ( $R^2 = 0.47$ ) and Co ( $R^2 = 0.96$ ). The positive correlation of REE and Y with Mg may be attributed to the fact that REE and Y tend to partition strongly into apatite, which commonly occurs as inclusions in clinopyroxene. This notion is supported by the relationship between REE-Y and P<sub>2</sub>O<sub>5</sub>, which show moderate (*e.g.*, Lu) to strong (*e.g.*, Eu) positive correlations ( $R^2 = 0.55–0.85$ ). The positive correlation of Mg with Co and Ni is also consistent with fractionation.

Trace elements for OPS, MS, ES and regional intrusions were normalized to primordial mantle (PM; Sun and McDonough, 1989) and plotted on a spider diagram in order to compare trends between the various rock types (Fig. 8). Figure 8 demonstrates that the OPS, MS, ES and regional intrusions are all significantly enriched in large-ion lithophile elements (LILE; Rb, Ba, K and Sr), Pb and U compared to high field-strength elements (HFSE), which is a characteristic of arc rocks (*e.g.*, Kamenetsky *et al.*, 1997; Coulson *et al.*, 1999). It can also be concluded that all intrusions show a similar pattern across the diagram, although some intrusions are more depleted in certain elements compared to others. Of note are the heavy rare earth elements (HREE), medium rare earth elements (MREE) and Ti, which are significantly more depleted in the OPS compared with the MS and regional intrusions. The disparity can be attributed to the partitioning of these elements into the phases augite, apatite and hornblende, and the higher modal abundance of these phases in the MS relative to the OPS.

A variety of metal abundances from samples of the BS and regional intrusions (Table 2) were plotted on bivariate diagrams to evaluate their covariance (Fig. 9). Rocks from the BS show positive correlations for Ag versus Cu ( $R^2 = 0.86$ ; Fig. 9A), Zn versus Pb ( $R^2 = 0.24$ ), Ni versus Co ( $R^2 = 0.50$ ) and Au versus As ( $R^2 = 0.69$ ; Fig. 9B). No correlation exists for Au versus Ag or Cu. With the exception of Ni versus Co, there are no correlations between the BS and regional intrusions. In the case of Pb versus Zn, however, the regional intrusions show a steeper positive trend compared to the BS. Moreover, when Zn/Pb is plotted against MgO, there is a single positive linear trend for all intrusions, which suggests that Zn was depleted relative to Pb with fractionation.

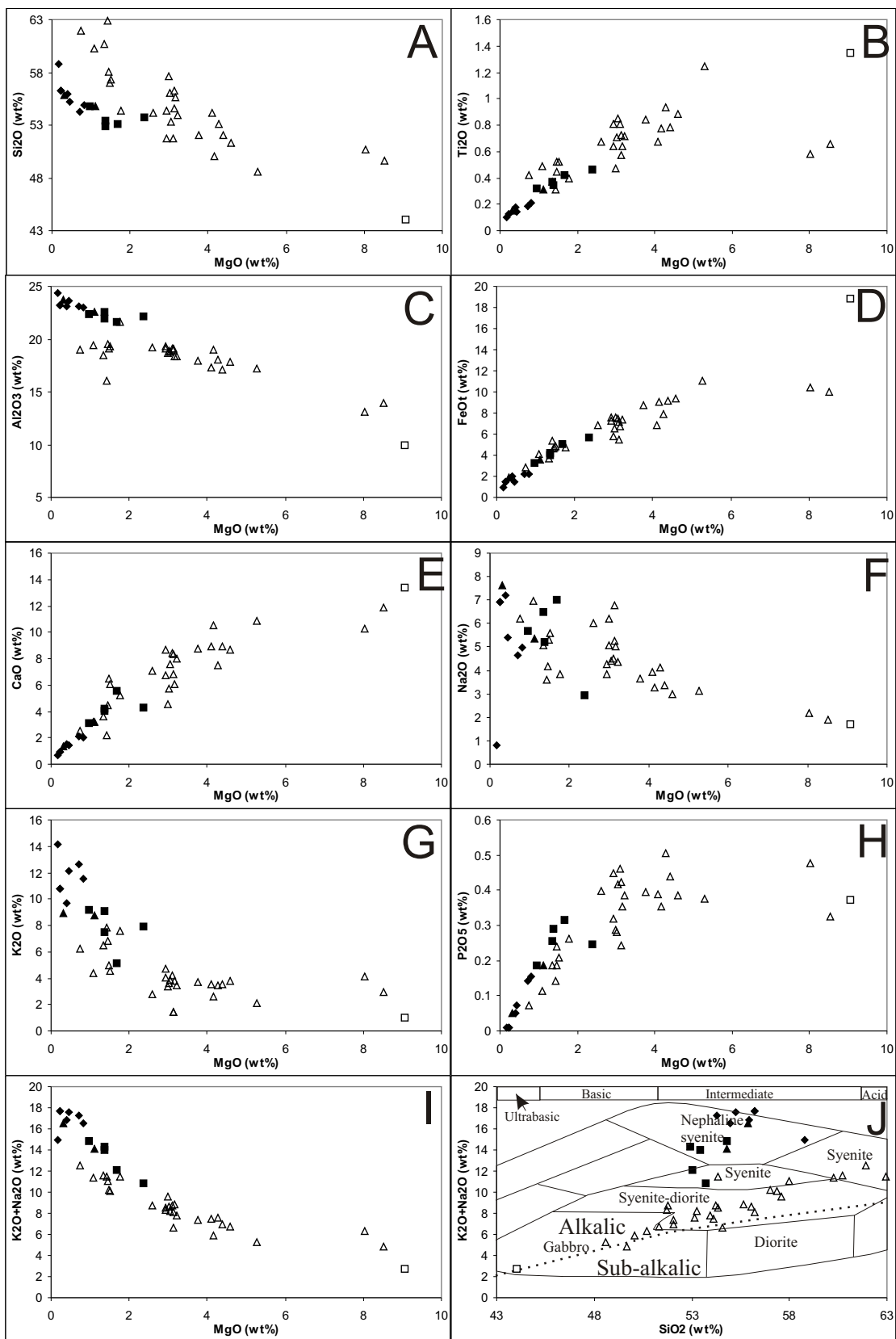


Figure 5. Major oxide bivalent diagrams for the Bootjack stock (MS, filled square; OPS, filled diamond; ES, filled triangle), regional intrusions (unfilled triangle) and a pyroxenite (sample MTP92-050 PX from Fraser, 1994). Part J is a total alkali versus silica (TAS) diagram. Note that the dotted line separates alkalic rocks from subalkalic rocks (after Wilson, 1989) and that all data are normalized to 100% anhydrous.

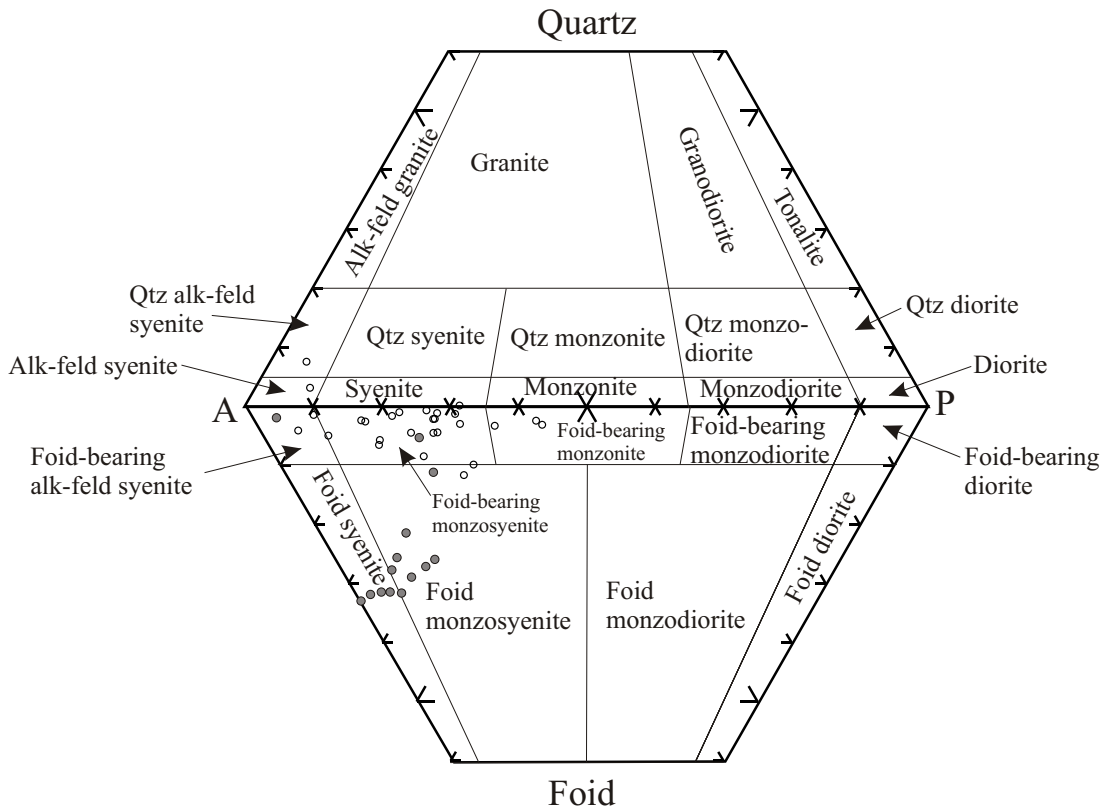


Figure 6. Rocks from the Bootjack stock (grey dots) and regional intrusions (colourless dots; see Table 1) plotted on an IUGS classification diagram using CIPW normative values. CIPW calculations were carried out using the same method as Le Maitre (1976). Note that BS rocks tend to plot in the Foid syenite to Foid monzosyenite field, compared with regional intrusions that plot mostly in the Foid-bearing monzosyenite field (after Streckeisen, 1976).

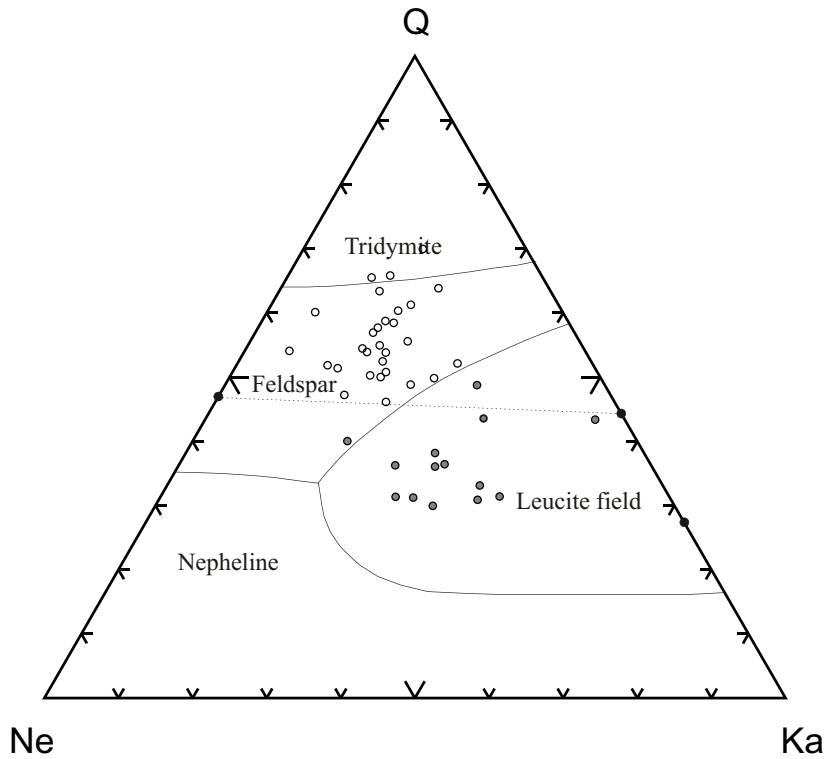


Figure 7. Rocks from the Bootjack stock and regional intrusions plotted on a nepheline-quartz-kalsilite (Ne-Q-Ka) diagram (assuming 1 Kb  $\text{PH}_2\text{O}$ ) using CIPW normative values that were calculated using the same method as Le Maitre (1976). Note that BS rocks tend to plot in the leucite field, whereas regional intrusions tend to plot in the feldspar field (after Rollinson, 1993).

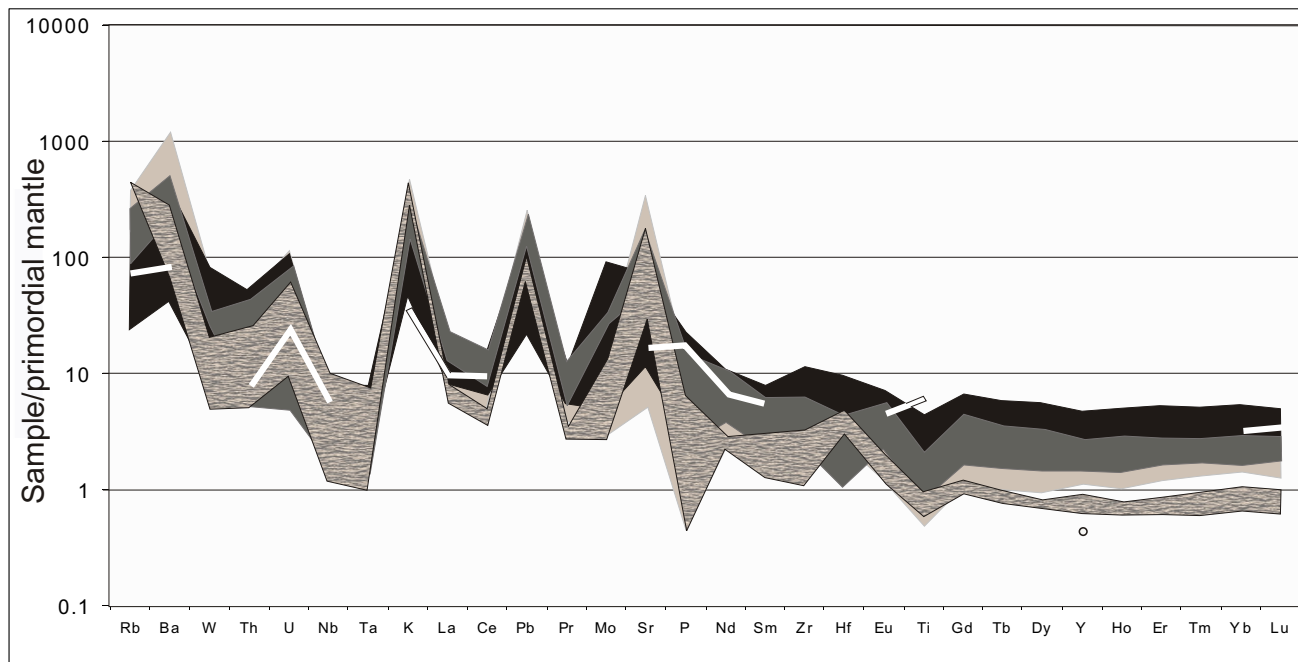


Figure 8. Spider diagram showing data from the Bootjack stock (MS, dark grey; ES, light grey; OPS, brick textured), regional intrusions (black) and Bootjack Lake pyroxenite (white line; sample MTP92-050PX from Fraser, 1994). All rocks are normalized to a primordial mantle (primordial mantle values from Sun and McDonough, 1989).

## DISCUSSION

### *Petrological and Geochemical Features of the Bootjack Stock*

Notably, one of the most significant aspects of the Bootjack stock (BS) is the existence of packed orbicular pseudoleucite syenite (OPS), which makes up an estimated 80% of the intrusion. Hence, an understanding of the genesis of pseudoleucite is particularly important with respect to understanding the BS. According to Deer *et al.* (1992), the genesis of pseudoleucite can be ascribed to two probable processes: 1) the breakdown of early-formed leucite with a Na-rich liquid; or 2) the breakdown of Na-rich leucite (or K-rich analcite) solid-solution series phase, which has been synthesized in experimental work. In natural systems, however, the composition of leucite does not depart significantly from the ideal formula ( $\text{KAISi}_2\text{O}_6$ ), and replacement of K by Na rarely exceeds 10% (Phillips and Griffen, 1981;

Deer *et al.*, 1992); alternatively, though, analcite containing up to 20% of leucite component in basalt has been reported (Deer *et al.*, 1992).

The geochemistry of four fresh samples from the OPS, each containing approximately 80–95% pseudoleucite, was examined in order to estimate the composition of the pseudoleucite constituent of the rock. Optically, all four samples have a matrix mineral assemblage that closely resembles the pseudoleucite constituent of the rock, with the exception of subordinate aegirine-augite and magnetite. Hence, whole rock data are believed to closely represent pseudoleucite geochemistry, with the exception of minor Na and Fe enrichment. Geochemical data for four OPS samples show Si/Al molar ratios close to two (average = 2.02; standard deviation = 0.032), which is consistent with the chemical formula for leucite, but Al/K molar ratios average 1.82 (st. dev. = 0.12), which is significantly greater than the ideal leucite formula (1:1). Molar ratios for Al/(K+Na) are close to 1:1 (*i.e.*, avg. = 1.07; st. dev. = 0.04), suggesting that either the alkali substitution of Na for K was

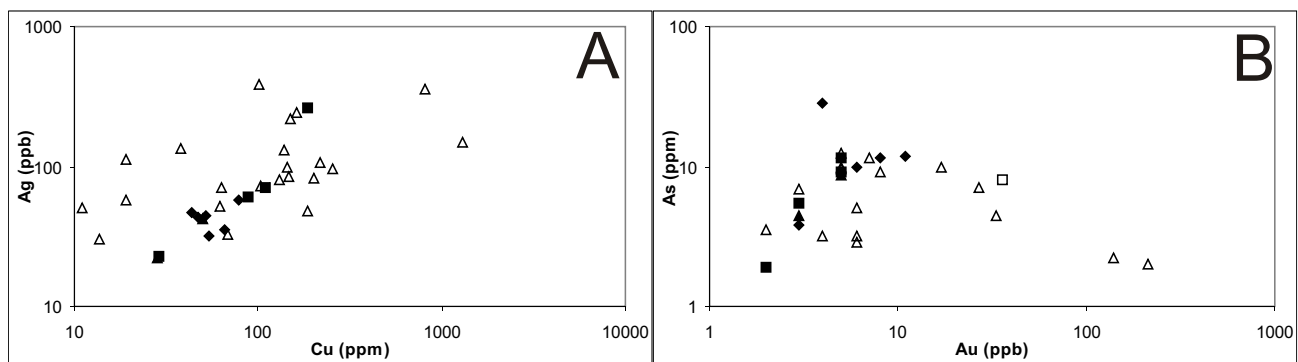


Figure 9. Bivariate diagrams for the Bootjack stock (MS, filled square; OPS, filled diamond; ES, filled triangle), regional intrusions (unfilled triangle) and Bootjack Lake pyroxenite (unfilled square; sample MTP92-050PX from Fraser, 1994).



and ABA05 41-336), h a y ne displays type 1 inclusions, which represent trapped sulphide melt. Hence, there is strong evidence to suggest that the residual Na-rich melt, which facilitated the breakdown of leucite, also contained significant amounts of Cu.

### **Geochemical and Petrographic Links Between H a y ne, Cu and Au**

The OPS samples containing the most interstitial h a y ne tend to have the highest concentration of Au and Na and a positive linear trend for Au versus Na, suggesting an intimate link between Au and a residual Na- and S-rich melt (Fig. 10A, C). In contrast no correlation is evident between Cu and Na. Moreover, those samples containing the most interstitial h a y ne tend to have lower concentrations of Cu and K (Fig. 10B, D). To explain this relationship, the authors suggest that h a y ne crystallized from a S and Na-rich residual melt that actively scavenged Cu (with S) and replaced K (with Na) as it moved through the crystal mush. Thus, those parts of the magma chamber that were more affected by the interstitial late-stage melt tend to have less Cu and K. For OPS rocks, there is a moderate positive correlation for Cu versus K, which is interpreted to be related to the affect of the residual melt.

From the relationship between K and Cu, it is possible to approximate how much Cu may have been lost as a result of leucite breakdown and Na exchange. Based on the known extent of the OPS (~10 km<sup>2</sup>) and assuming a thickness of 300 m, the loss of Cu from the OPS as a result of S scavenging is estimated to be approximately 156 000 t (see Fig. 10E). This calculation for Cu loss from the BS is not significantly different from estimated total Cu reserves and total Cu production at Mount Polley (Imperial Metals Corporation, 2004). However, the calculation is considered to be a minimum estimate, given that the absolute extent of the BS is poorly constrained and the likelihood that the overall loss of Cu (as well as Au and Ag) from the BS may have been significantly greater based on the high concentration of these metals in cogenetic, less evolved alkali basalt (see Logan and Bath, 2006), which likely resembles the composition of the parental melt for the BS.

### **Emplacement and Differentiation of the BS**

The BS is a zoned intrusive body that is characterized by an OPS and ES core and an MS rim. The authors infer that the mafic-rich rim is a product of differentiation, where mafic phases accumulated along the walls of the intrusion. This idea is supported by the relative density of the mafic phases and the existence of cumulate layering at certain outcrops. Conversely, the OPS is interpreted to represent the accumulation of leucite crystals. Given the relatively low density of leucite (specific gravity = 2.47–2.50; Deer *et al.*, 1992), it is suggested that leucite, on crystallizing, floated to the top of the magma chamber and accumulated at the carapace of the intrusion (similar conclusion to Coulson *et al.* [1999] for Zippa Mountain). The ES is considered to be a late component of the system, as it is seen to crosscut the MS; however, it has not been observed to cut the OPS. The occurrence of pegmatitic texture within the ES, and also within local regions of the OPS, suggests that volatiles likely accumulated in the core of the magma chamber beneath the leucite layer and were then released as local pulses.

## **CONCLUSIONS**

- Rocks from the Bootjack stock (BS) show geochemical fractionation trends, similar to those of coeval intrusions from the Mount Polley complex, Bullion pit, Shiko Lake and QR mine, that suggest a cogenetic relationship. However, the BS is more fractionated compared to other intrusions.
- Rocks from the orbicular pseudoleucite syenite (OPS) have Si/Al molar ratios that are close to 2, and Al/(Na+K) ratios of close to 1, which is consistent to that of leucite when Na for K substitution is taken into account. The transition from leucite to pseudoleucite occurred by the introduction of Na-rich melt, which is evident from the presence of interstitial h a y ne.
- The presence of sulphide melt inclusions within interstitial h a y ne from the BS is primary evidence of a Cu-rich sulphide melt, concentrated in a residual S and Na-rich melt, that could have migrated through the intrusive body and accumulated at the carapace of the intrusion along with magmatic volatiles and metals.
- The generation of excess K as a result of leucite breakdown to pseudoleucite may explain the pervasive early K alteration in the rocks at Mount Polley, whereas the late-stage S and Na-rich residual melt may represent the later Na alteration at Mount Polley.
- Further study on h a y ne is required in order to accurately determine its crystal chemistry and the composition of type 2 inclusions (sulphate, silicate or carbonate?). These studies may help to establish whether an intimate link exists between the BS and mineralization at Mount Polley.
- As shown by Frei (1996), testing the ratio of oxidized and reduced sulphur in bulk rock as well as individual minerals (*e.g.*, apatite) can be an important indicator for distinguishing barren from mineralized intrusions. The authors wonder if unaltered h a y ne from the BS could also be used as a tool for tracing the oxidation state of S, given the high concentration of S in its structure and its ability to readily host both S<sup>6+</sup> and S<sup>2-</sup>.

## **ACKNOWLEDGMENTS**

First and foremost, we would like to thank the Mount Polley geology team of Pat McAndless, Chris Reese, Lee Ferreira, Leif Bjornson, Jacqueline Blackwell, Chris Taylor and Sheila Jonnes for bending over backwards for us this summer. Their efforts made this project much easier and we sincerely thank them. We would also like to genuinely thank Ray Lett for his help and advice with the geochemistry. Graham Nixon, George Simandl and Vadim Kamenetsky are all thanked for freely offering their time to discuss some of our queries.

## **REFERENCES**

- Bailey, D.G. and Archibald, D.A. (1990): Age of the Bootjack stock, Quesnel Terrane, south-central British Columbia (93A); in Geological Fieldwork 1989, *BC Ministry of Energy, Mines and Petroleum Resources*, Paper 1990-1, pages 79–82.

- Coulson, I.M., Russell, J.K. and Dipple, G.M. (1999): Origins of the Zippa Mountain pluton: a late Triassic, arc-derived, ultrapotassic magma from the Canadian Cordillera; *Canadian Journal of Earth Sciences*, Volume 36, no 9, pages 1415–1434.
- Deer, W.A., Howie, R.A. and Zussman, J. (1992): An Introduction to the Rock-Forming Minerals (2nd Edition); Longman.
- Fraser, T.M. (1994): Geology, alteration and origin of hydrothermal breccias at the Mount Polley alkalic porphyry copper-gold deposit, south-central British Columbia; M.Sc. thesis, University of British Columbia, Vancouver, BC, 261 pages.
- Frei, R. (1996): Sulfur in bulk rock and igneous apatite: tracing mineralized and barren trends in intrusions; *Schweizerische Mineralogische Und Petrographische Mitteilungen*, Volume 76, no 1, pages 57–73.
- Hodgson, C.J., Bailes, R.J. and Versoza, R.S. (1976): Cariboo-Bell; in *Porphyry Deposits of the Canadian Cordillera*, Sunderland Brown, A., Editor, *Canadian Institute of Mining and Metallurgy*, Special Volume 15, pages 388–396.
- Imperial Metals Corporation (2004): Mount Polley's Northeast zone expanded and mine restart economics robust; *Imperial Metals Corporation*, press release, August 3, 2004, URL < <http://www.imperialmetals.com/s/News-2004.asp?ReportID=85638&Type=News-Release-2004&Title=Mount-Polleys-Northeast-Zone-Expanded-and-Mine-Restart-Economics-Robust> > [09/12/2005].
- Kamenetsky, V.S., Crawford, A.J., Eggins, S. and Muhe, R. (1997): Phenocryst and melt inclusion chemistry of near-axis seamounts, Valu Fa Ridge, Lau Basin: insight into mantle wedge melting and the addition of subduction components; *Earth and Planetary Science Letters*, Volume 151, no 3–4, pages 205–223.
- Le Maitre, R.W. (1976): The chemical variability of some common igneous rocks; *Journal of Petrology*, Volume 17, pages 589–637.
- Logan, J.M. and Bath, A.B. (2006): Geochemistry of the Nicola group basalts from Quesnel, at the latitude of Mount Polley; in *Geological Fieldwork 2005*, *BC Ministry of Energy, Mines and Petroleum Resources*, Paper 2006-1 and *Geoscience BC*, Report 2006-1.
- Logan, J.M. and Mihalynuk, M.G. (2005): Regional geology and setting of the Cariboo, Bell, Springer and Northeast porphyry Cu-Au zones at Mount Polley, south-central British Columbia; in *Geological Fieldwork 2004*, *BC Ministry of Energy, Mines and Petroleum Resources*, Paper 2005-1, pages 249–270.
- Mortensen, J.K., Ghosh, D.K. and Ferri, F. (1995): U-Pb geochronology of intrusive rock associated with copper-gold porphyry deposits in the Canadian Cordillera; in *Porphyry Deposits of the Northwestern Cordillera of North America*, Schroeter, T.G., Editor, *Canadian Institute of Mining and Metallurgy*, Special Volume 46, pages 142–158.
- Mortimer, N. (1987): The Nicola Group: Late Triassic and Early Jurassic subduction-related volcanism in British Columbia; *Canadian Journal of Earth Sciences*, Volume 24, pages 2521–2536.
- Mortimer, N., Van Der Heyden, P., Armstrong, R.L. and Harakal, J. (1990): U-Pb and K-Ar dates related to the timing of magmatism and deformation in the Cache Creek Terrane and Quesnellia, southern British Columbia; *Canadian Journal of Earth Sciences*, Volume 27, pages 117–123.
- Panteleyev, A., Bailey, D.G., Bloodgood, M.A. and Hanckock, K.D. (1996): Geology and mineral deposits of the Quesnel River – Horsefly map area, central Quesnel Trough, British Columbia (NTS 93A/5, 6, 7, 11, 12, 13; 93B/9, 16; 93G/1; 93H/4); *BC Ministry of Energy, Mines and Petroleum Resources*, Bulletin 97, 156 pages.
- Phillips, W.R. and Griffen, D.T. (1981): *Optical Mineralogy: The Nonopaque Minerals*; W.H. Freeman and Co., San Francisco, California, 677 pages.
- Rollinson, H.R. (1993): *Using Geochemical Data: Evaluation, Presentation, Interpretation*; Prentice Hall, 352 pages.
- Streckeisen, A. (1976): To each plutonic rock its proper name; *Earth Science Reviews*, Volume 12, pages 1–33.
- Sun, S.S. and McDonough, W.F. (1989): Chemical and isotopic systematics of oceanic basalts: implications for mantle composition and processes; in *Magmatism in Ocean Basins*, Saunders, A.D. and Norry, M.J., Editors, *Geological Society of London*, Special Publication 42, pages 313–345.
- Wheeler, J.O. and McFeely, P. (1991): Tectonic assemblage map of the Canadian Cordillera and adjacent parts of the United States of America; *Geological Survey of Canada*, Map 1712A, scale 1:2 000 000.
- Wilson, M. (1989): *Igneous Petrogenesis*; Unwin Hyman, London, United Kingdom, 466 pages.

